

Quantum-Dot Spin Qubit and Hyperfine Interaction

D. Klauser, W. A. Coish and Daniel Loss

Department of Physics and Astronomy, University of Basel, Klingelbergstrasse 82, CH-4056 Basel, Switzerland

Abstract. We review our investigation of the spin dynamics for two electrons confined to a double quantum dot under the influence of the hyperfine interaction between the electron spins and the surrounding nuclei. Further we propose a scheme to narrow the distribution of difference in polarization between the two dots in order to suppress hyperfine induced decoherence.

1 Introduction

The fields of semiconductor physics and electronics have been successfully combined for many years. The invention of the transistor meant a revolution for electronics and has led to significant development of semiconductor physics and its industry. More recently, the use of the spin degree of freedom of electrons, as well as the charge, has attracted great interest [1]. In addition to applications for spin electronics (spintronics) in conventional devices, for instance based on the giant magneto-resistance effect [2] and spin-polarized field-effect transistors [3], there are applications that exploit the quantum coherence of the spin. Since the electron spin is a two-level system, it is a natural candidate for the realization of a quantum bit (qubit) [4]. A qubit is the basic unit of information in quantum computation. The confinement of electrons in semiconductor structures like quantum dots allows for better control and isolation of the electron spin from its environment. Control and isolation are important issues to consider for the design of a quantum computer.

Formally, a quantum computation is performed through a set of transformations, called gates [5]. A gate applies a unitary transformation U to a set of qubits in a quantum state $|\Psi\rangle$. At the end of the calculation, a measurement is performed on the qubits (which are in the state $|\Psi'\rangle = U|\Psi\rangle$). There are many ways to choose sets of universal quantum gates. These are sets of gates from which any computation can be constructed, or at least approximated as precisely as desired. Such a set allows one to perform any arbitrary calculation without inventing a new gate each time. The implementation of a set of universal gates is therefore of crucial importance. It can be shown

* Presented as plenary talk at the annual DPG meeting 2006, Dresden (to appear in Advances in Solid State Physics vol. 46, 2006).

that it is possible to construct such a set with gates that act only on one or two qubits at a time [6].

The successful implementation of a quantum computer demands that some basic requirements be fulfilled. These are known as the DiVincenzo criteria [7] and can be summarized in the following:

1. *Information storage—the qubit:* We need to find some quantum property of a scalable physical system in which to encode our bit of information, that lives long enough to enable us to perform computations.
2. *Initial state preparation:* It should be possible to set the state of the qubits to 0 before each new computation.
3. *Isolation:* The quantum nature of the qubits should be tenable; this will require enough isolation of the qubit from the environment to reduce the effects of decoherence.
4. *Gate implementation:* We need to be able to manipulate the states of individual qubits with reasonable precision, as well as to induce interactions between them in a controlled way, so that the implementation of gates is possible. Also, the gate operation time τ_s has to be much shorter than the decoherence time T_2 , so that $\tau_s/T_2 \ll r$, where r is the maximum tolerable error rate for quantum error correction schemes to be effective.
5. *Readout:* It must be possible to measure the final state of our qubits once the computation is finished, to obtain the output of the computation.

To construct quantum computers of practical use, we emphasize that the scalability of the device should not be overlooked. This means it should be possible to enlarge the device to contain many qubits, while still adhering to all requirements described above. It should be mentioned here that this represents a challenging issue in most of the physical setups proposed so far.

2 Quantum-Dot Spin Qubit

The requirement for scalability motivated the Loss-DiVincenzo proposal [4] for a solid-state quantum computer based on electron spin qubits.

The qubits of the Loss-DiVincenzo quantum computer are formed from the two spin states ($|\uparrow\rangle, |\downarrow\rangle$) of a confined electron. The considerations discussed in this proposal are generally applicable to electrons confined to any structure, such as atoms, molecules, etc., although the original proposal focuses on electrons localized in quantum dots. These dots are typically generated from a two-dimensional electron gas (2DEG), in which the electrons are strongly confined in the vertical direction. Lateral confinement is provided by electrostatic top gates, which push the electrons into small localized regions of the 2DEG (see Fig. 1). Initialization of the quantum computer can be achieved by allowing all spins to reach their thermodynamic ground state at low temperature T in an applied magnetic field B (i.e., virtually all spins

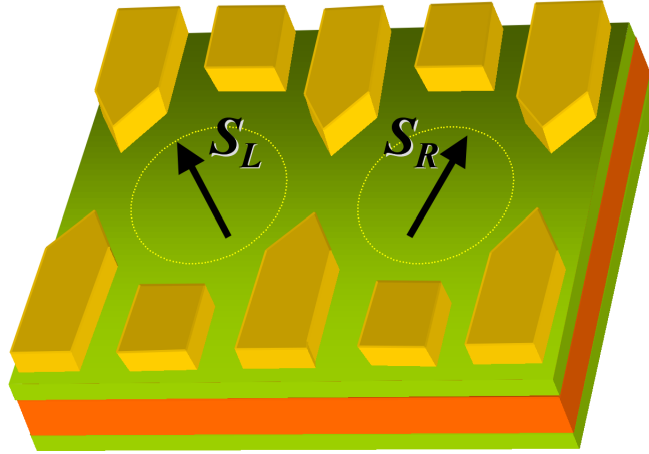


Fig. 1. Two neighbouring electron spins confined to quantum dots, as in the Loss-DiVincenzo proposal. The lateral confinement is controlled by top gates. A time-dependent Heisenberg exchange coupling $J(t)$ can be pulsed high by pushing the electron spins closer, generating an appreciable overlap between the neighbouring orbital wave functions.

will be aligned if the condition $|g\mu_B B| \gg k_B T$ is satisfied, with g -factor g , Bohr magneton μ_B , and Boltzmann's constant k_B). Single-qubit operations can be performed, in principle, by changing the local effective Zeeman interaction at each dot individually. To do this may require large magnetic field gradients [8], g -factor engineering [9], magnetic layers, the inclusion of nearby ferromagnetic dots [4], polarized nuclear spins, or optical schemes.

In the Loss-DiVincenzo proposal, two-qubit operations are performed by pulsing the electrostatic barrier between neighboring spins. When the barrier is high, the spins are decoupled. When the inter-dot barrier is pulsed low, an appreciable overlap develops between the two electron wave functions, resulting in a non-zero Heisenberg exchange coupling J . The Hamiltonian describing this time-dependent process is given by

$$H(t) = J(t) \mathbf{S}_L \cdot \mathbf{S}_R. \quad (1)$$

This Hamiltonian induces a unitary evolution given by the operator $U = \mathcal{T} \exp \{-i \int H(t) dt / \hbar\}$, where \mathcal{T} is the time-ordering operator. If the exchange is pulsed on for a time τ_s such that $\int J(t) dt / \hbar = J_0 \tau_s / \hbar = \pi$, the states of the two spins, with associated operators \mathbf{S}_L and \mathbf{S}_R , as shown in figure 1, will be exchanged. This is the SWAP operation. Pulsing the exchange for the shorter time $\tau_s/2$ generates the “square-root of SWAP” operation, which can be used in conjunction with single-qubit operations to generate the controlled-NOT (quantum XOR) gate [4]. The “square-root of SWAP” gate has recently been implemented in an experiment by Petta *et al.* [10] with a

switching time $\tau_s = 180$ ps. For scalability, and application of quantum error correction procedures in any quantum computing proposal, it is important to turn off inter-qubit interactions in the idle state. In the Loss-DiVincenzo proposal, this is achieved with exponential accuracy since the overlap of neighboring electron wave functions is exponentially suppressed with increasing separation. A detailed investigation of decoherence during gating due to a bosonic environment was performed in the original work of Loss and DiVincenzo. Since then, there have been many studies of leakage and decoherence in the context of the quantum-dot quantum computing proposal.

In addition to the interaction-based gate operations introduced above, it has been shown recently [11, 12] that it is also possible to generate the controlled-NOT based on partial Bell state (parity) measurements.

For both interaction-based and measurement-based quantum computation with the quantum-dot spin qubit, decoherence due to the coupling of the qubit to its environment is a major obstacle. There are two important sources of decoherence in GaAs quantum dots: spin-orbit coupling (interaction between spin and charge fluctuations) and hyperfine coupling (interaction between the electron spin and nuclear spins). In the case of spin-orbit interaction alone it has been shown that the decoherence time T_2 (which is the relevant timescale for quantum computing tasks) exceeds the relaxation time T_1 and is given by $T_2 = 2T_1$ to leading order in the spin-orbit coupling [13]. Since the T_1 obtained in measurements [14, 15] is on the order of ms, but the ensemble-averaged dephasing time T_2^* measured is ~ 10 ns, spin-orbit interaction is not limiting for the dephasing time T_2^* . The limiting source of decoherence is the hyperfine interaction [10].

3 Hyperfine Interaction in Single and Double Dots

The hyperfine interaction between the electron spin and the nuclear spins present in all III-V semiconductors [16] leads to the strongest decoherence effect [10, 17, 18, 19, 20, 21, 22, 23, 24]. Experiments [10, 25, 26, 27] have yielded values for the free-induction spin dephasing time T_2^* that are consistent with $T_2^* \sim \sqrt{N}/A \sim 10$ ns [20, 21, 22] for $N = 10^6$, $\hbar = 1$, and $A = 90\mu\text{eV}$ in GaAs, where N is the number of nuclei within one quantum dot Bohr radius and A characterizes the weighted average hyperfine coupling strength in GaAs [28]. This is to be contrasted with potential spin-echo envelope decay times, which may be much longer [23, 29, 30, 31]. With a two-qubit switching time of $\tau_s \sim 180$ ps [10] this only allows $\sim 10^2$ gate operations within T_2^* , which falls short (by a factor of 10 to 10^2) of current requirements for efficient quantum error correction [32].

There are several ways to overcome the problem of hyperfine-induced decoherence, of which measurement and thus projection of the nuclear spin state may be the most promising [23]. Other methods include polarization [17, 22, 23, 33] of the nuclear spins and spin echo techniques [10, 23, 30].

However, in order to extend the decay time by an order of magnitude through polarization of the nuclear spins, a polarization of above 99% is required [23], but the best result so far reached is only $\sim 60\%$ in quantum dots [25]. With spin-echo techniques, gate operations still must be performed within the single-spin free-induction decay time, which requires faster gate operations. A projective measurement of the nuclear spin state leads to an extension of the free-induction decay time for the spin. This extension is only limited by the ability to do a strong measurement since the longitudinal nuclear spin in a quantum dot is expected to survive up to the spin diffusion time, which is on the order of seconds for nuclear spins surrounding donors in GaAs [34].

A detailed analysis of the spin dynamics for one electron in a single quantum dot can be found in Ref.[23]. Here we concentrate on the case of two electrons in a double quantum dot. The spin \mathbf{S}_l of an electron in quantum dot $l = 1, 2$, interacts with the surrounding nuclear spins \mathbf{I}_k via the Fermi contact hyperfine interaction:

$$H_{\text{hf}} = \mathbf{S}_l \cdot \mathbf{h}_l; \quad \mathbf{h}_l = \sum_k A_k^l \mathbf{I}_k; \quad A_k^l = v_0 A |\psi^l(\mathbf{r}_k)|^2, \quad (2)$$

where v_0 is the volume of a crystal unit cell containing one nuclear spin. The effective Hamiltonian in the subspace of one electron on each dot is best written in terms of the sum and difference of electron spin and collective nuclear spin operators: $\mathbf{S} = \mathbf{S}_1 + \mathbf{S}_2$, $\delta\mathbf{S} = \mathbf{S}_1 - \mathbf{S}_2$ and $\mathbf{h} = \frac{1}{2}(\mathbf{h}_1 + \mathbf{h}_2)$, $\delta\mathbf{h} = \frac{1}{2}(\mathbf{h}_1 - \mathbf{h}_2)$:

$$H_{\text{eff}}(t) = \epsilon_z S^z + \mathbf{h} \cdot \mathbf{S} + \delta\mathbf{h} \cdot \delta\mathbf{S} + \frac{J(t)}{2} \mathbf{S} \cdot \mathbf{S} - J(t), \quad (3)$$

where $\epsilon_z = g\mu_B B$ is the Zeeman splitting induced by an applied magnetic field $\mathbf{B} = (0, 0, B)$, $B > 0$. We assume that the Zeeman splitting is much larger than $\langle \delta\mathbf{h} \rangle_{\text{rms}}$ and $\langle \mathbf{h}_i \rangle_{\text{rms}}$, where $\langle \mathcal{O} \rangle_{\text{rms}} = \langle \psi_I | \mathcal{O}^2 | \psi_I \rangle^{1/2}$ is the root-mean-square expectation value of the operator \mathcal{O} with respect to the nuclear spin state $|\psi_I\rangle$. Under these conditions the relevant spin Hamiltonian becomes block diagonal with blocks labeled by the total electron spin projection along the magnetic field S^z . In the subspace of $S^z = 0$ the Hamiltonian can be written as ($\hbar = 1$) [24, 35]

$$H_0(t) = \frac{J(t)}{2} \tau^x - \frac{1}{2} \Omega \tau^z; \quad J(t) = J_0 + j \cos(\omega t), \quad \Omega = 2(\delta h^z + \delta b^z). \quad (4)$$

Here, δb^z is the inhomogeneity of an externally applied classical static magnetic field with $\delta b^z \ll B$. The Pauli matrices τ^α , $\alpha = x, y, z$ are given in the basis of $|+\rangle \equiv |\tau^z = 1\rangle = |\downarrow\uparrow\rangle$ and $|-\rangle \equiv |\tau^z = -1\rangle = |\uparrow\downarrow\rangle$.

The dynamics of the two-electron spin states depends strongly on the initial state of the nuclear spin system. We denote by $|n\rangle$ the eigenstates of δh^z with $\delta h^z |n\rangle = \delta h_n^z |n\rangle$. If the initial state of the nuclear spin system is $\rho_I(0) = |n\rangle \langle n|$ and if we neglect spin-flip processes (as can be done for a large enough magnetic field B), then the initial spin state of the electron

does not decay. Thus, if it is possible to prepare the nuclear spin system in an eigenstate $|n\rangle$, hyperfine-induced decoherence could be overcome. In general, however, the initial state of the nuclear spin system is not an eigenstate $|n\rangle$ but a general mixture:

$$\rho_I(0) = \sum_i p_i |\psi_I^i\rangle \langle \psi_I^i|; \quad |\psi_I^i\rangle = \sum_n a_n^i |n\rangle, \quad (5)$$

where the a_n^i satisfy the normalization condition $\sum_n |a_n^i|^2 = 1$ and $\sum_i p_i = 1$. We denote by $\rho_I(n) = \sum_i p_i |a_n^i|^2$ the diagonal elements of the nuclear spin density operator.

For a large number of nuclear spins $N \gg 1$ which are in a superposition of δh^z -eigenstates $|n\rangle$, $\rho_I(n)$ describes a continuous Gaussian distribution of δh_n^z values, with mean $\overline{\delta h^z}$ and variance $\sigma^2 = (\overline{\delta h^z} - \overline{\delta h^z})^2$. In the limit of large N , the approach to a Gaussian distribution for a sufficiently randomized nuclear system is guaranteed by the central limit theorem [23]. We perform the continuum limit according to

$$\sum_n \rho_I(n) f(n) \rightarrow \int dx \rho_I(x) f(x); \quad \rho_I(x) = \frac{1}{\sqrt{2\pi}\sigma} \exp\left(-\frac{(x - x_0)^2}{2\sigma_0^2}\right), \quad (6)$$

where $x = \delta h_n^z + \delta b^z$, $x_0 = \overline{\delta h^z} + \delta b^z$ and $\sigma_0^2 = \overline{x^2} - x_0^2$.

For the case of a static exchange interaction $J(t) = J_0$, the decay of the two-electron spin states in the $S^z = 0$ subspace due to the Gaussian distribution of nuclear spin states may be calculated in several interesting limits [24, 35]. Assuming the initial state of the two-electron system is $\rho_e(0) = |+\rangle\langle +|$, the probability P^+ to measure the $|+\rangle$ state as a function of time is given by

$$P_{J=J_0}^+(t) = \int_{-\infty}^{\infty} \rho_I(x) \left(\frac{1}{2} + \frac{2x^2}{s(x)^2} + \frac{J^2}{2s(x)^2} \cos(s(x)t) \right) \quad (7)$$

with $s(x) = \sqrt{J^2 + 4x^2}$. In the limit $\sigma_0 \rightarrow 0$, which corresponds to one fixed eigenvalue, there is no decay. However, for $\sigma_0 > 0$ there is decay. For the regime $|x_0| \gg \sigma_0$ we have a Gaussian decay at short times with a decay time $t_0 \sim 1/\sigma_0$:

$$P_{J=J_0}^+(t) \approx \frac{1}{2} + \frac{2x_0^2}{\omega_0^2} + \left(\frac{1}{2} - \frac{2x_0^2}{\omega_0^2} \right) \exp\left(-\frac{t^2}{2t_0^2}\right) \cos(\omega_0 t), \quad (8)$$

$$\omega_0 = \sqrt{J^2 + 4x_0^2}, \quad t_0 = \frac{\omega_0}{4|x_0|\sigma_0}; \quad |x_0| \gg \sigma_0, \quad t \ll \frac{\omega_0^{3/2}}{2J^2\sigma_0^2}. \quad (9)$$

Thus, decreasing σ_0 increases the coherence time t_0 . Hence, the strategy to suppress hyperfine-induced decoherence is to narrow the Gaussian distribution of nuclear spin eigenvalues through a measurement of the eigenvalue of δh^z , i.e., of the difference in polarization between the two dots [23, 24]. It has also been proposed to measure the nuclear spin polarization using a phase

estimation method [36]. In the ideal case, phase estimation yields one bit of information about the nuclear spin system for each perfectly measured electron. Optical methods have also been proposed [37]. The all-electrical method we propose here can be applied with current technology used in Refs. [10, 27].

4 Nuclear Spin State Narrowing

The general idea behind state narrowing is that the evolution of the two-electron system is dependent on the collective nuclear spin state and thus knowing the evolution of the two-electron system determines the nuclear spin state.

The eigenstates of the Hamiltonian H_0 are product states: if the nuclear spin system is in an eigenstate $|n\rangle$ of δh^z with $\delta h^z |n\rangle = \delta h_n^z |n\rangle$, we have $H|\psi\rangle = H_n|\psi_e\rangle \otimes |n\rangle$, where in H_n the operator δh^z has been replaced by δh_n^z and $|\psi_e\rangle$ is the electron spin part of the wave function. Thus, in the Hamiltonian for the evolution of the initial two-electron system, the parameter δh_n^z is determined by the state of the nuclear spin system. Initializing the two-electron system to the $|+\rangle$ state, i.e., $\rho_e(0) = |+\rangle\langle+|$ and performing a measurement in the $|\pm\rangle$ basis at time t_m yields for the distribution of nuclear spin eigenvalues (which is the diagonal part of the nuclear spin density operator in the continuum limit) after the measurement [35]

$$\rho_I^{(1,+,\omega)}(x) = \rho_I(x)(1 - L_\omega(x))\frac{1}{P_\omega^+}, \quad (10)$$

$$\rho_I^{(1,-,\omega)}(x) = \rho_I(x)L_\omega(x)\frac{1}{P_\omega^-}, \quad (11)$$

where $\rho_I(x)$ is the initial Gaussian distribution of nuclear spin eigenvalues (see Eq. (6)) and the probabilities P^\pm for measuring $|\pm\rangle$ are given by

$$P_\omega^+ = \int_{-\infty}^{\infty} dx \rho_I(x)(1 - L_\omega(x)), \quad (12)$$

$$P_\omega^- = \int_{-\infty}^{\infty} dx \rho_I(x)L_\omega(x), \quad (13)$$

with

$$L_\omega(x) = \frac{1}{2} \frac{(j/4)^2}{(x - \frac{\omega}{2})^2 + (j/4)^2}. \quad (14)$$

To obtain this result we have assumed that the measurement is performed with low time resolution [38] $\Delta t \gg 1/j$ and that the parameters satisfy the requirements given in Eq. (15) below. The distribution of nuclear spin eigenvalues after the measurement depends on the result of the measurement (whether $|+\rangle$ or $|-\rangle$ was measured) and on the driving frequency ω of the oscillating exchange interaction $J(t)$. In the case where the measurement outcome is $|+\rangle$, the initial distribution $\rho_I(x)$ is multiplied by $1 - L_\omega(x)$ which

causes a dip in $\rho_I(x)$ at $x = \omega/2$. However, in the case where the result of the measurement was $|-\rangle$, the initial distribution $\rho_I(x)$ is multiplied by $L(x)$. The full-width at half-maximum (FWHM) of $L_\omega(x)$ is $j/2$, i.e., half the amplitude of the applied oscillation exchange interaction $J(t)$. Thus, choosing $j < \sigma_0$, $\rho_I^{(1,-,\omega)}(x)$ is dominated by the Lorentzian and therefore the FWHM of the initial nuclear spin distribution has been narrowed by a factor $\approx j/4\sigma_0$. The probability P_ω^- to measure $|-\rangle$ in the regime $j \ll \sigma_0$ is given by $P_\omega^- \approx (j/6\sigma_0) \exp((x_0 - \omega/2)^2/2\sigma_0^2)$ and the nuclear spin distribution after measuring $|-\rangle$ is centered around $\omega/2$. Thus, through such a measurement it is possible to choose the center of the nuclear spin distribution by choosing the driving frequency. However, the larger the difference $x_0 - \omega/2$, the smaller is the probability to have measurement outcome $|-\rangle$, which leads to narrowing.

4.1 Experimental Recipe

An experimental implementation of this scheme of course requires the ability to initialize to the state $|+\rangle$ and to read-out the states $|\pm\rangle$. This has recently been achieved in an experiment by Petta *et al.* [10] using adiabatic passage from the $S^z = 0$ singlet. What needs to be achieved in addition is to apply an external magnetic field gradient δb^z between the two dots in order to satisfy the requirements on the parameters of the system:

$$J_0 \ll x_0, \quad j \ll x_0, \quad \sigma_0 \ll x_0, \quad j < \sigma_0. \quad (15)$$

Typical values for the parameters satisfying these requirements are: $1/\sigma_0 = 10$ ns, $1/j = 100$ ns, $\omega = 2x_0 = 10^9 - 10^{10}$ Hz.

The pulse-sequence for one measurement is shown in Fig. 2. The parameter ϵ describes the detuning between the singlet state with two electrons on the right dot and the singlet state with one electron on each dot: $\epsilon = E_{S(0,2)} - E_{S(1,1)}$. First the system is set to the $S(1,1)$ from the $S(0,2)$ state by going from large positive to negative detuning ϵ (such that still $J \gg |x_0|$) as described in Ref. [10] (rapid adiabatic passage through $S(1,1) - T_+$ resonance). In the limit of $J \ll |x_0|$ and $x_0 > 0$, the ground state is $|+\rangle$ (for $x_0 < 0$, the ground state is $|-\rangle$ and $|\pm\rangle$ thus need to be interchanged in the following description) and initialization to $|+\rangle$ is thus possible by adiabatic passage from $S(1,1)$, i.e., by switching adiabatically to large negative detuning (such that $J \ll x_0$). Then the oscillating signal is applied to $J(t)$ for a time t_m . Finally we adiabatically switch back to $J \gg x_0$. With this the $|+\rangle$ state goes to the singlet $S(1,1)$, and the $|-\rangle$ state goes to the $S^z = 0$ triplet $T_0(1,1)$. Read-out of the singlet and triplet may then be achieved via switching to large positive detuning: the $S(1,1)$ state goes over to the $S(0,2)$ while the $T_0(1,1)$ does not since tunneling preserves spin. The number of electrons on the right dot can then be detected via a charge sensor (QPC). If the outcome of the measurement is $|-\rangle$, we have achieved narrow-

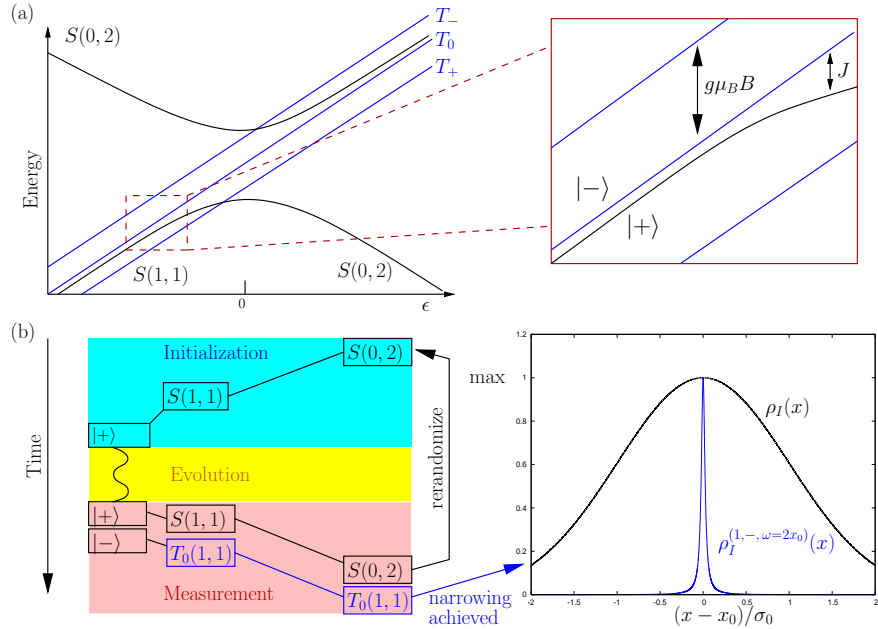


Fig. 2. In this figure the pulse-sequence for one measurement in the basis $|\pm\rangle$ is explained. (a) The level diagram for the two-electron spin states (sweeping $\epsilon = E_{S(1,1)} - E_{S(0,2)}$ with $E_{S(1,1)} + E_{S(0,2)}$ held constant). Inset: The splitting between the $S(1,1)$ and T_0 state is given by the exchange interaction J between the two dots. For $J \rightarrow 0$ the $|\pm\rangle$ states become eigenstates. (b) The change of the detuning ϵ during the course of the measurement is sketched: the position of the boxes corresponds to the value of ϵ . After applying the oscillating signal the system is in either one of $|\pm\rangle$, which results in a different state when switching back to positive detuning. If the system ends up in the T_0 state (which corresponds to measurement result $|-\rangle$) narrowing has been achieved, otherwise the nuclear system must be rerandomized and the measurement repeated.

ing. In the case where we have measured $|+\rangle$, the nuclear spin distribution is rerandomized and the measurement is repeated.

4.2 Adaptive scheme

If measurements at several different driving frequencies can be performed, a systematic narrowing of the distribution can be achieved by an adaptive scheme. Such an adaptive scheme is more intricate than the one described above, but allows one to narrow by more than a factor $j/4\sigma_0$.

The results of Eqs. (10,11) may be generalized to the case of M subsequent measurements at different driving frequencies ω_i under the assumption, that the nuclear spin system is static between subsequent measurements:

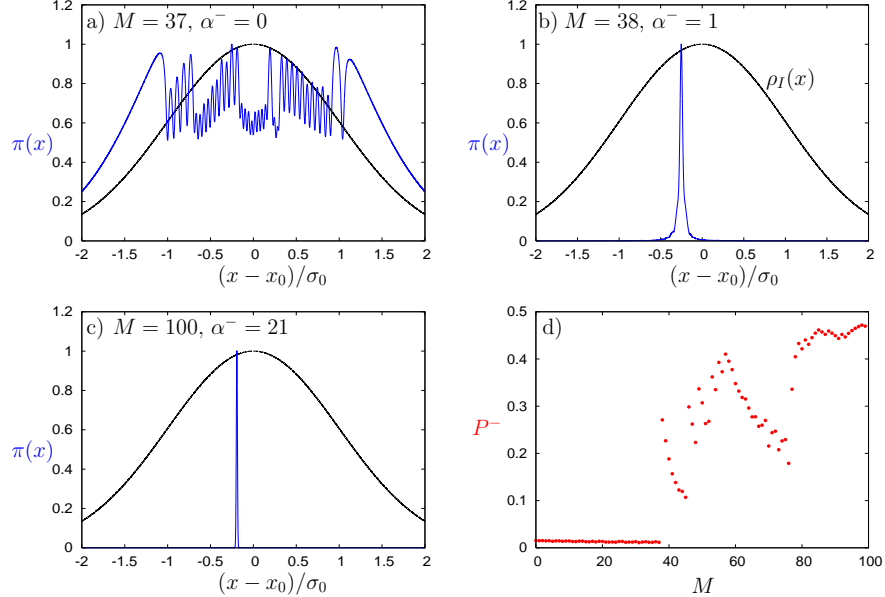


Fig. 3. In this figure we show a typical [39] sequence of the rescaled probability density of eigenvalues $\pi(x) = \rho_I^{(M, \{\alpha_i^-\}, \{\omega_i\})}(x) / \max(\rho_I^{(M, \{\alpha_i^-\}, \{\omega_i\})}(x))$ for the adaptive scheme. Here, $\rho_I^{(M, \{\alpha_i^-\}, \{\omega_i\})}(x)$ is given in Eq.(16). We have $x = \delta h_n^z + \delta b^z$, $j/\sigma_0 = 1/10$, $\alpha^- = \sum_{i=1}^M \alpha_i^-$, and in a)–c) the initial Gaussian distribution (with FWHM $2\sigma_0\sqrt{2\ln 2} \approx 2\sigma_0$) is plotted for reference. a) Up to $M = 37$ measurements the outcome is never $|-\rangle$ and thus each measurement “burns a hole” into the distribution where it previously had its maximum. b) In the 38th measurement the outcome is $|-\rangle$ which leads to a narrowed distribution of nuclear spin eigenvalues (peak centered at ≈ -0.25) with a FWHM that is reduced by a factor $\approx j/4\sigma_0$. c) Adapting the driving frequency ω to this peak, i.e., setting $\omega/2 = x_{\max}$ in subsequent measurements, leads to further narrowing every time $|-\rangle$ is measured. In this example the final FWHM is $\approx \sigma_0/100$, i.e., the distribution has been narrowed by a factor $\approx j/10\sigma_0$. d) The probability P^- to measure $|-\rangle$ jumps up after the 38th measurement and after $|-\rangle$ is measured several more times, this probability saturates close to 1/2.

$$\rho_I^{(M, \{\alpha_i^-\}, \{\omega_i\})}(x) = \frac{\rho_I(x)}{Q(\{\alpha_i^-\}, \{\omega_i\})} \prod_{i=1}^M L_{\omega_i}^{\alpha_i^-} (1 - L_{\omega_i})^{1-\alpha_i^-}, \quad (16)$$

where $Q(\{\alpha_i^-\}, \{\omega_i\})$ is the normalization factor, $\alpha_i^- = 1$ for measurement outcome $|-\rangle$ and $\alpha_i^- = 0$ for measurement outcome $|+\rangle$ in the i^{th} measurement with driving frequency ω_i . Further, $\{\omega_i\} = \{\omega_1, \dots, \omega_M\}$ and $\{\alpha_i^-\} = \{\alpha_1^-, \dots, \alpha_M^-\}$. As we have seen in the case of just one measurement, it is the measurement outcome $|-\rangle$ that leads to narrowing. Thus,

before each measurement ω_i is chosen to maximize the probability $P_{\omega_i}^-$ to measure $|-\rangle$. The reason that ω_i must be adapted and that one should not keep measuring at the same driving frequency is that the measurement outcome $|+\rangle$ causes a dip in $\rho_I(x)$ at the position where $L_{\omega_i}(x)$ has its peak and since $P_{\omega_i}^-$ is the overlap of $\rho_I(x)$ and $L_{\omega_i}(x)$, this causes $P_{\omega_i}^-$ to diminish with each measurement.

To see what is a typical measurement history for such an adaptive scheme we have performed simulations. The results for a typical [39] sequence of measurements is shown in Fig. 3 (for another sequence see Fig.2 in Ref. [35]).

5 Conclusions

We have reviewed our scheme that uses pseudospin measurements in the $S^z = 0$ subspace of two electron spin states in a double quantum dot to narrow the distribution of difference in nuclear polarization between the two dots. A successful experimental implementation of this scheme would allow to suppress hyperfine-induced decoherence and thus to reach the coherence times required for efficient quantum error correction.

Acknowledgements

We thank G. Burkard, M. Duckheim, J. Lehmann, F. H. L. Koppens, D. Stepanenko and, in particular, A. Yacoby for useful discussions. We acknowledge financial support from the Swiss NSF, the NCCR nanoscience, EU NoE MAGMANet, DARPA, ARO, ONR, JST ICORP, and NSERC of Canada.

References

1. D. D. Awschalom, D. Loss, and N. Samarth, *Semiconductor Spintronics and Quantum Computing* (Springer-Verlag, Berlin, 2002).
2. M. N. Baibich, J. M. Broto, A. Fert, F. Nguyen van Dau, F. Petroff, P. Etienne, G. Creuzet, A. Friederich, and J. Chazelas, Phys. Rev. Lett. **61**, 2472 (1988).
3. S. Datta and B. Das, Appl. Phys. Lett. **56**, 665 (1990).
4. D. Loss and D. P. DiVincenzo, Phys. Rev. A **57**, 120 (1998).
5. J. Preskill, <http://theory.caltech.edu/people/preskill/ph229/>.
6. A. Barenco, C. H. Bennett, R. Cleve, D. P. DiVincenzo, N. Margolus, P. Shor, T. Sleator, J. A. Smolin, and H. Weinfurter, Phys. Rev. A **52**, 3457 (1995).
7. D. P. DiVincenzo, D. Bacon, J. Kempe, G. Burkard, and K. B. Whaley, Nature **408**, 339 (2000).
8. L.-A. Wu, D. A. Lidar, and M. Friesen, Phys. Rev. Lett. **93**, 030501 (2004).
9. G. Medeiros-Ribeiro, E. Ribeiro, and H. Westfahl, Applied Physics A: Materials Science & Processing **77**, 725 (2003).

10. J. R. Petta, A. C. Johnson, J. M. Taylor, E. A. Laird, A. Yacoby, M. D. Lukin, C. M. Marcus, M. P. Hanson, and A. C. Gossard, *Science* **309**, 2180 (2005).
11. H.-A. Engel and D. Loss, *Science* **309**, 586 (2005).
12. C. W. Beenakker, D. P. DiVincenzo, C. Emery, and M. Kindermann, *Phys. Rev. Lett.* **93**, 020501 (2004).
13. V. N. Golovach, A. V. Khaetskii, and D. Loss, *Phys. Rev. Lett.* **93**, 016601 (2004).
14. J. M. Elzerman, R. Hanson, L. H. Willems van Beveren, B. Witkamp, L. M. K. Vandersypen, and L. P. Kouwenhoven, *Nature* **430**, 431 (2004).
15. M. Kroutvar, Y. Ducommun, D. Heiss, M. Bichler, D. Schuh, G. Abstreiter, and J. J. Finley, *Nature* **432**, 81 (2004).
16. J. Schliemann, A. Khaetskii, and D. Loss, *J. Phys.: Condens. Matter* **15**, 1809 (2003).
17. G. Burkard, D. Loss, and D. P. DiVincenzo, *Phys. Rev. B* **59**, 2070 (1999).
18. S. I. Erlingsson, Y. V. Nazarov, and V. I. Fal'ko, *Phys. Rev. B* **64**, 195306 (2001).
19. S. I. Erlingsson and Y. V. Nazarov, *Phys. Rev. B* **66**, 155327 (2002).
20. A. V. Khaetskii, D. Loss, and L. Glazman, *Phys. Rev. Lett.* **88**, 186802 (2002).
21. I. A. Merkulov, A. L. Efros, and M. Rosen, *Phys. Rev. B* **65**, 205309 (2002).
22. A. Khaetskii, D. Loss, and L. Glazman, *Phys. Rev. B* **67**, 195329 (2003).
23. W. A. Coish and D. Loss, *Phys. Rev. B* **70**, 195340 (2004).
24. W. A. Coish and D. Loss, *Phys. Rev. B* **72**, 125337 (2005).
25. A. S. Bracker, E. A. Stinnett, D. Gammon, M. E. Ware, J. G. Tischler, A. Shabaev, A. L. Efros, D. Park, D. Gershoni, V. L. Korenev, and I. A. Merkulov, *Phys. Rev. Lett.* **94**, 047402 (2005).
26. M. V. Dutt, J. Cheng, B. Li, X. Xu, X. Li, P. R. Berman, D. G. Steel, A. S. Bracker, D. Gammon, S. E. Economou, R.-B. Liu, and L. J. Sham, *Phys. Rev. Lett.* **94**, 227403 (2005).
27. F. H. L. Koppens, J. A. Folk, J. M. Elzerman, R. Hanson, L. H. W. van Beveren, I. T. Vink, H. P. Tranitz, W. Wegscheider, L. P. Kouwenhoven, and L. M. K. Vandersypen, *Science* **309**, 1346 (2005).
28. D. Paget, G. Lampel, B. Sapoval, and V. I. Safarov, *Phys. Rev. B* **15**, 5780 (1977).
29. R. de Sousa and S. Das Sarma, *Phys. Rev. B* **67**, 033301 (2003).
30. N. Shenvi, R. de Sousa, and K. B. Whaley, *Phys. Rev. B* **71**, 224411 (2005).
31. W. Yao, R.-B. Liu, and L. J. Sham, arXiv:cond-mat/0508441 (2005).
32. A. M. Steane, *Phys. Rev. A* **68**, 042322 (2003).
33. A. Imamoğlu, E. Knill, L. Tian, and P. Zoller, *Phys. Rev. Lett.* **91**, 017402 (2003).
34. D. Paget, *Phys. Rev. B* **25**, 4444 (1982).
35. D. Klauser, W. A. Coish, and D. Loss, arXiv:cond-mat/0510177 (Phys. Rev. B in press) (2005).
36. G. Giedke, J. M. Taylor, D. D'Alessandro, M. D. Lukin, and A. Imamoğlu, arXiv:quant-ph/0508144 (2005).
37. D. Stepanenko, G. Burkard, G. Giedke, and A. Imamoğlu, *Phys. Rev. Lett.* **96**, 136401 (2006).
38. This assumption is not necessary for our narrowing scheme. However, it does allow for the derivation of the analytical formulas in this section, which give insight into the mechanism of narrowing.
39. We have performed more than 60 runs of the simulation, varying M and j/σ_0 .